ISSN: 0256-307X

中国物理快报
Chinese Physics Letters

Volume 27 Number 9 September 2010

A Series Journal of the Chinese Physical Society
Distributed by IOP Publishing

Online: http://www.iop.org/journals/cpl
http://cpl.iphy.ac.cn

CHINESE PHYSICAL SOCIETY

Effects of Perpendicular Thermal Velocities on the Transverse Instability in Electron Phase Space Holes *

WU Ming-Yu(吴明雨)[1], WU Hong(吴洪)[1,2], LU Quan-Ming(陆全明)[1**], XUE Bing-Sen(薛炳森)[3]

[1]*CAS Key Laboratory of Basic Plasma Physics, School of Earth and Space Sciences, University of Science and Technology of China, Hefei 230026*

[2]*Department of Physics, School of Sciences, Jimei University, Xiamen 361021*

[3]*Space Weather Operation and Research Division, China Meteorology Administration, Beijing 100081*

(Received 31 May 2010)

A multi-dimensional electron phase-space hole (electron hole) is considered to be unstable to the transverse instability. We perform two-dimensional (2D) particle-in-cell (PIC) simulations to study the evolutions of electron holes in weakly magnetized plasma ($\Omega_e < \omega_{pe}$, where Ω_e and ω_{pe} are the electron gyrofrequency and plasma frequency, respectively), and the effects of perpendicular thermal velocities on the transverse instability are investigated. The transverse instability can cause decay of the electron holes. We find that with the increasing perpendicular thermal velocity tending to stabilize the transverse instability, the corresponding wave numbers decrease.

PACS: 52.35.Sb, 52.65.Rr DOI: 10.1088/0256-307X/27/9/095201

Electron phase-space holes (electron holes) have been observed in different space environments, such as the auroral region, the magnetotail, the transition region of the bow shock, the solar wind, the magnetopause, and the magnetosheath.[1−6] They have also been observed in laboratory plasma, for example, in a magnetized plasma surrounded by a waveguide and an unmagnetized laser-generated plasma.[7,8] Electron holes are considered to be stationary Bernstein–Greene–Kruskal (BGK) solutions of the Vlasov and Poisson equations.[9−11] They are positive potential pulses, and the parallel cut of their parallel electric field $E_{||}$ has bipolar structures. Particle-in-cell (PIC) simulations have confirmed that electron holes can be formed during the nonlinear evolution of electron bi-stream instabilities, and these holes can persist for a sufficiently long time in one-dimensional (1D) PIC simulations.[10,12−14] Recently, Muschietti *et al.*[15] proposed that electron holes are unstable to the transverse instability in weakly magnetized plasma, which is due to the dynamics of the trapped electrons in the electron holes. Perturbations in electron holes can produce transverse gradients of the electric potential. Such transverse gradients focus the trapped electrons into regions that already have a surplus of electrons, which results in larger transverse gradients and more focusing. Lastly, the transverse instability occurs. Based on the combined actions of the transverse instability and the stabilization of the background magnetic field, Lu *et al.*[16] successfully explained the unipolar structures of the parallel cut of the perpendicular electric field $E_\perp$ in electron holes, which have been observed by Polar and FAST satellite.[1,17]

In this Letter, we perform two-dimensional (2D) particle-in-cell (PIC) simulations to study the evolutions of electron holes in weakly magnetized plasma ($\Omega_e < \omega_{pe}$, where Ω_e and ω_{pe} are the electron gyrofrequency and plasma frequency, respectively). The effects of perpendicular thermal velocities on the transverse instability have also been investigated in Muschietti *et al.*[15] They fixed the wave number of the transverse instability by adding an initial perturbation, and found that the transverse tends to be stabilized with the increase of the electron perpendicular thermal velocity. In our study, we perform PIC simulations to investigate the transverse instability in electron holes without adding any initial perturbations, and the transverse instability grows spontaneously. Therefore, the effects of the electron perpendicular thermal velocities on the wave numbers of the transverse instability can be studied.

A 2D electrostatic PIC code under periodic boundary conditions is employed in our simulations.[18,19] The background magnetic field $\boldsymbol{B}_0$ is along the x direction. In the simulations, we only move electrons, while ions are motionless and form a neutralizing background. Initially, a potential structure, which represents an electron hole, is located in the middle of the simulation domain. The potential structure is described as

$$\phi(x) = \psi \exp[-0.5(x-L)^2/\Delta_{||}^2], \qquad (1)$$

*Supported by the National Natural Science Foundation of China under Grant Nos 40974081, 40971053 and 40725013, the Knowledge Innovation Project of Chinese Academy of Sciences under Grant No KJCX2-YW-N28, and the Specialized Research Fund for State Key Laboratories.

**To whom correspondence should be addressed. Email: qmlu@ustc.edu.cn

where $\Delta_{||}$ and L are the half width and center position of the electron hole, respectively, ψ is the amplitude of the potential structure. The potential structure is homogeneous in the transverse direction. The trapped electrons gyrate in the background magnetic field, simultaneously they bounce back and forth in the parallel direction of the electron hole. The motions of a trapped electron are determined by the ratio of the electron gyrofrequency Ω_e to the bounce frequency $\omega_b = \sqrt{\psi/\Delta_{||}^2}$.[15] The initial electron distributions can be calculated by the BGK method self-consistently, which has already been given by Muschietti *et al.*[20] It is

$$F(x, v_x, v_y, v_z) = F_1(w)\exp[-0.5(v_y^2 + v_z^2)/T_{\perp e}], \quad (2)$$

where $T_{\perp e}$ is the electron perpendicular temperature, $w \equiv v_x^2 - 2\phi(x)$ is twice the parallel energy and

$$F_1(w) = \frac{\sqrt{-w}}{\pi\Delta_{||}^2}\left[1 + 2\ln\left(\frac{\psi}{-2w}\right)\right] + \frac{6 + \left(\sqrt{2} + \sqrt{-w}\right)(1-w)\sqrt{-w}}{\pi(\sqrt{2} + \sqrt{-w})(4 - 2w + w^2)} \quad \text{for} \quad -2\psi \le w < 0, \quad (3a)$$

$$F_1(w) = \frac{6\sqrt{2}}{\pi(8 + w^3)} \quad \text{for} \quad w > 0. \quad (3b)$$

Equations (3a) and (3b) describe the distributions of the trapped and passing electrons, respectively. The trapped electron distribution has a hollowed out shape, while the passing electron distribution has a flattop shape.

In the simulations, the density is normalized to the unperturbed density n_0. The velocities are expressed in units of the electron parallel thermal velocity $v_{||\mathrm{Te}} = (T_{||e}/m_e)^{1/2}$. The dimensionless units used here have space in Debye length $\lambda_D = \left(\frac{\varepsilon_0 T_{||e}}{n_0 e^2}\right)^{1/2}$, time in the inverse plasma frequency $\omega_{pe} = (\frac{n_0 e^2}{m_e \varepsilon_0})^{1/2}$, and potential in $\frac{m_e v_{||\mathrm{Te}}^2}{e}$. Cell size units $\lambda_D \times \lambda_D$ are used in the simulations, and the time step is $0.02\omega_{pe}^{-1}$. There are average 625 particles in each cell, and the number of cells is 128×512. Ω_e is chosen to be $0.1\omega_{pe}$. The initial potential is characterized by $\psi = 0.8$ and $\Delta_{||} = 2.0$. Initially, the electrons are loaded to satisfy Eqs. (2) and (3). We change the perpendicular thermal velocity $v_{\perp\mathrm{Te}}$ to investigate its effect on the transverse instability.

Figure 1 shows the simulation results for $v_{\perp\mathrm{Te}} = 1.0v_{||\mathrm{Te}}$. The top row displays the time evolution of the electric field energies (a1) E_x^2 and (b1) E_y^2, respectively, and they are normalized by $n_0T_{||e}/\varepsilon_0$. From the second row, the left and right columns plot the electric field component E_x and E_y at $\omega_{pe}t = 0$, 70 and 160 in the domain $0 \le x \le 128\lambda_D$ and $0 \le y \le 128\lambda_D$. With the excitation of the transverse instability at about $\omega_{pe}t = 40$, the electric field energy E_x^2 begins to decrease and E_y^2 increases. Then, a kinked electron hole can be found in the simulation domain, and the bipolar structures of the parallel of E_y can be observed if we cut the electron hole along the direction parallel to the background magnetic field. After the transverse instability is sufficiently strong, it begins to destroy the electron hole. At about $\omega_{pe}t = 80$ both the electric field component E_x and E_y begin to decrease until they disappear at about $\omega_{pe}t = 150$.

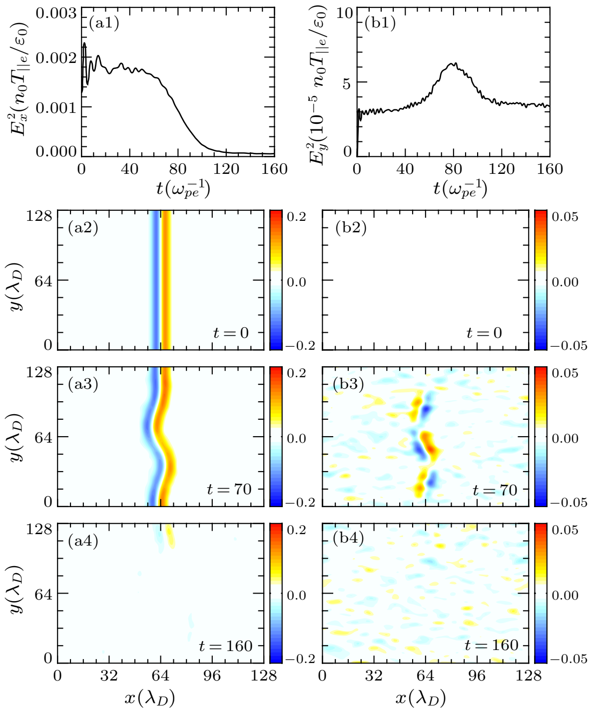

Fig. 1. The simulation results for $v_{\perp\mathrm{Te}} = 1.0v_{||\mathrm{Te}}$. The top row shows the time evolution of the electric field energies E_x^2 and E_y^2, respectively, and they are normalized by $n_0T_{||e}/\varepsilon$. From the second row, the left and right columns plot the electric field component (a) E_x and (b) E_y at $\omega_{pe}t = 0$, 70 and 160 in the domain $0 \le x \le 128\lambda_D$ and $0 \le y \le 128\lambda_D$.

The transverse instability is a self-focusing type of instability acting at the level of the trajectories of trapped electron in electron holes. This can be illustrated by following electron trajectories in a kinked electron hole, whose potential is modeled as[15]

$$\varphi(x, y) = \psi\exp\left[-0.5\left(\frac{x - 16.0 - \varepsilon\Delta_{||}\cos ky}{\Delta_{||}}\right)^2\right], \quad (4)$$

where ε is a measure of the perturbation and k is its transverse wave number. The parameters are $\psi = 0.8$, $\Delta_{||} = 2.0$, $\varepsilon = 0.3$ and $k = 0.39$. Figure 2 describes the typical trajectories of trapped electrons in the electron hole. The charged density ρ is also shown in the figure. Initially, these electrons are distributed evenly in the

y direction, and they start from $x = 13$. The trapped electrons tend to accumulate to the regions that already have a surplus of electrons (with negative charge density). Then, the transverse undulation in the electron hole becomes more and more pronounced, which results in a self-focusing type of instability.

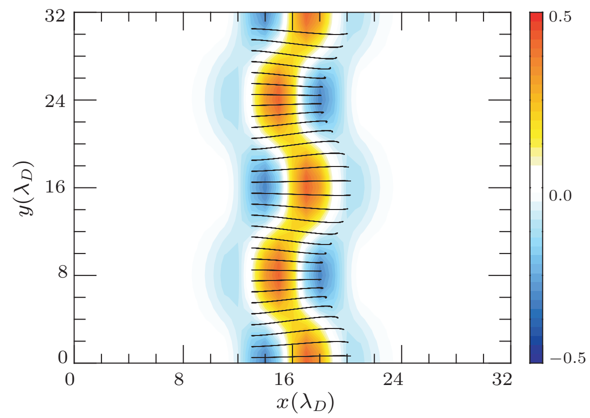

Fig. 2. The typical trajectories of trapped electrons in the electron hole. The charged density ρ is also shown. Initially, these electrons are distributed evenly in the y direction, and they start from $x = 13$. In the figure, the solid lines denote the typical trajectories of trapped electrons, and the color representations denote the charged density ρ. The parameters are $\psi = 0.8$, $\Delta_{||} = 2.0$, $\varepsilon = 0.3$ and $k = 0.39$.

Figure 3 shows the time evolution of the electric field energies E_x^2 and E_y^2 for $v_{\perp \rm Te} = 0.2$, 0.5 and $1.0v_{||\rm Te}$, respectively. The electric field energies are normalized by $n_0T_{||e}/\varepsilon_0$. In the figure, the increase of the electric field energy E_y^2 means the excitation of the transverse instability in the electron hole, and correspondingly, the electric field energy E_x^2 decreases. Therefore, we can find that with the increase of the electron perpendicular thermal velocity, the transverse instability is difficult to be excited. The transverse instability begins to be excited at about $\omega_{pe}t = 24$, 32, and 40 for $v_{\perp \rm Te} = 0.2$, 0.5 and $1.0v_{||\rm Te}$, respectively, at the same time, E_y^2 attains their maximum values (about 0.00031, 0.00013, and 0.00006, respectively) at $\omega_{pe}t = 45$, 65, and 80.

The reasons for the stabilization of the electron perpendicular thermal velocity to the transverse instability in electron holes can be explained as follows: with the increase of the perpendicular thermal velocity, the diffusion across the background magnetic field also increases. It can prevent the trapped electrons from being focused by the transverse gradients of the potential, and make the electron hole stable. At the same time, as pointed out by Muschitti *et al.*,[15] the criterion for the transverse instability in electron holes is $v_{\perp \rm Te} \ll \omega_b/k$. In this study, we find that with the increase of the perpendicular thermal velocity $v_{\perp \rm Te}$, the wave numbers k of the transverse instability decreases. This can be demonstrated in Fig. 4, in which we plot the wave numbers k of the kinked electron holes at different perpendicular thermal velocities. The wave numbers are calculated from the self-consistent PIC simulations without initial perturbations when the kinked electron holes are fully developed. The wave numbers k are inversely proportional to the perpendicular thermal velocity $v_{\perp \rm Te}$ and consistent with the criterion of the transverse instability proposed by Muschitti *et al.*[15]

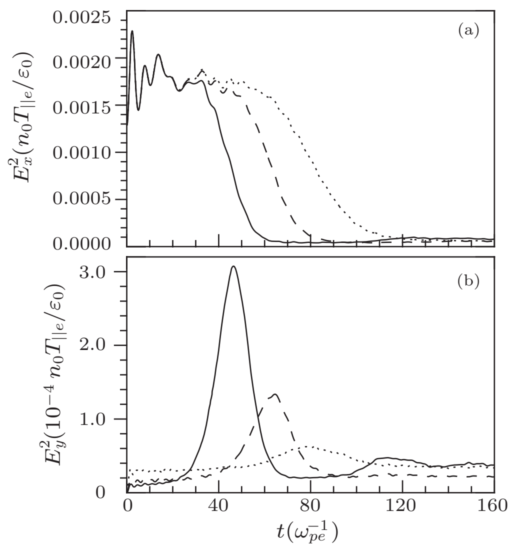

Fig. 3. The time evolution of the electric field energies (a) E_x^2 and (b) E_y^2 for $v_{\perp \rm Te} = 0.2$, 0.5 and $1.0v_{||\rm Te}$, respectively. The solid, dashed, and dotted lines denote $0.2v_{||\rm Te}$, $0.5v_{||\rm Te}$ and $1.0v_{||\rm Te}$, respectively. Here the electric field energies are normalized by $n_0T_{||e}/\varepsilon$.

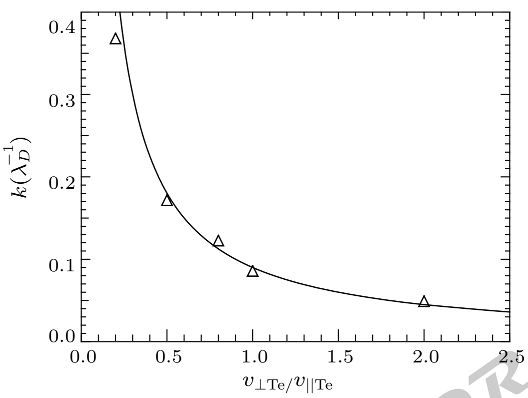

Fig. 4. The wave number k of the kinked electron holes formed due to the transverse instability for $v_{\perp \rm Te} = 0.2$, 0.5, 0.8, 1.0, $2.0v_{||\rm Te}$. The triangles are the results from 2D PIC simulations. The solid lines represent the equation $k = av_{\perp \rm Te}^{-1}$, where $a = 0.09$.

In summary, performing 2D electrostatic PIC simulations we have investigated the transverse instability electron holes in weakly magnetized plasma under different electron perpendicular thermal velocity conditions. Our results show that the transverse instability causes the electron holes to become kinked, and lastly destroys the electron holes. At the same time, the increase of the electron perpendicular thermal velocity tends to stabilize it, and the corresponding wave numbers decrease. Weibel or whistler instability is also unstable to electron anisotropic temperature.[21−23] However, its effects are neglected because it is an electromagnetic instability and we use electrostatic PIC simulations in the present study. The interactions between the transverse instability and Weibel instability in electron holes are our investigation in the future.

References

[1] Ergun R E et al 1998 *Geophys. Res. Lett.* **25** 2041
[2] Matsumoto H et al 1994 *Geophys. Res. Lett.* **21** 2915
[3] Bale S D et al 1998 *Geophys. Res. Lett.* **25** 2929
[4] Mangeney A et al 1999 *Ann. Geophys.* **17** 307
[5] Cattell C et al 2002 *Geophys. Res. Lett.* **29** 1065
[6] Pickett J S et al 2004 *Ann. Geophys.* **22** 2525
[7] Saeki K et al 1979 *Phys. Rev. Lett.* **42** 501
[8] Sarri G et al 2010 *Phys. Plasmas* **17** 010701
[9] Bernstein I B et al 1957 *Phys. Rev.* **108** 546
[10] Schamel H 1986 *Phys. Rep.* **140** 161
[11] Ng C S and Bhattacharjee A 2005 *Phys. Rev. Lett.* **95** 245004
[12] Omura Y et al 1994 *Geophys. Res. Lett.* **21** 2923
[13] Lu Q M et al 2005 *J. Geophys. Res.* **110** A03223
[14] Lu Q M et al 2005 *Phys. Plasmas* **12** 072903
[15] Muschietti L et al 2000 *Phys. Rev. Lett.* **85** 94
[16] Lu Q M et al 2008 *J. Geophys. Res.* **113** A11219
[17] Franz J R et al 1998 *Geophys. Res. Lett.* **25** 1277
[18] Decyk V K 1995 *Comput. Phys. Commun.* **87** 87
[19] Lu Q M and Cai D S 2001 *Comput. Phys. Commun.* **135** 93
[20] Muschietti L et al 1999 *Geophys. Res. Lett.* **26** 1093
[21] Weibel E S 1959 *Phys. Rev. Lett.* **2** 83
[22] Lu Q M et al 2004 *Chin. Phys. Lett.* **21** 129
[23] Lu Q M, Zhou L H and Wang S 2010 *J. Geophys. Res.* **115** A02213

Chinese Physics Letters

Volume 27 Number 9 2010

GENERAL

090201 **New Type Soliton Solutions to Korteweg-de Vries and Benjamin–Bona–Mahony Equations**
LIU Yu

090202 **Effect of Geometric Distance on Agreement Dynamics of Naming Game**
HAO Jia-Bo, YANG Han-Xin, LIU Run-Ran, WANG Bing-Hong, ZHANG Zhi-Yuan

090203 **An Application of a Generalized Version of the Dressing Method to Integration of a Variable-Coefficient Dirac System**
SU Ting, WANG Zhi-Wei

090301 **A New Quantum Key Distribution Scheme Based on Frequency and Time Coding**
ZHU Chang-Hua, PEI Chang-Xing, QUAN Dong-Xiao, GAO Jing-Liang, CHEN Nan, YI Yun-Hui

090302 **Wigner Functions for the Bateman System on Noncommutative Phase Space**
HENG Tai-Hua, LIN Bing-Sheng, JING Si-Cong

090303 **Testing Evolution Equation for Entanglement of Two-Qubit Systems in Noisy Channels on Ensemble Quantum Computers**
ZHANG Han, LUO Jun, REN Ting-Ting, SUN Xian-Ping

090304 **A New Approach for Constructing New Coherent-Entangled State Representations**
MA Shan-Jun, XU Xue-Xiang

090305 **From the Thermo Wigner Operator to the Thermo Husimi Operator in Thermo Field Dynamics**
XU Xue-Fen, ZHU Shi-Qun

090306 **Entanglement of Superpositions of Orthogonal Maximally Entangled States**
ZHANG Dao-Hua, ZHOU Duan-Lu, FAN Heng

090307 **Cryptanalysis and Improvement of Two GHZ-State-Based QSDC Protocols**
GUO Fen-Zhuo, QIN Su-Juan, WEN Qiao-Yan, ZHU Fu-Chen

090501 **Analytical Approach to Space- and Time-Fractional Burgers Equations**
Ahmet Yıldırım, Syed Tauseef Mohyud-Din

090502 **Thermodynamic Performance Characteristics of an Irreversible Micro-Brownian Heat Engine Driven by Temperature Difference**
ZHANG Yan-Ping, HE Ji-Zhou

090503 **Chaotic System Identification Based on a Fuzzy Wiener Model with Particle Swarm Optimization**
LI Yong, TANG Ying-Gan

090504 **Fast-Scale and Slow-Scale Subharmonic Oscillation of Valley Current-Mode Controlled Buck Converter**
ZHOU Guo-Hua, XU Jian-Ping, BAO Bo-Cheng, ZHANG Fei, LIU Xue-Shan

090505 **Bosons or Fermions in 1D Power Potential Trap with Repulsive Delta Function Interaction**
MA Zhong-Qi, C. N. Yang

090506 **Stochastic Resonance in a Time-Delayed Bistable System Driven by Square-Wave Signal**
GUO Feng, ZHOU Yu-Rong, ZHANG Yu

NUCLEAR PHYSICS

092101 **Effects of Pairing Correlations on Formation of Proton Halo in ^{9}C**
HAN Rui, LI Jia-Xing, YAO Jiang-Ming, JI Juan-Xia, WANG Jian-Song, HU Qiang

(Continued on inside back cover)

092501 **Elastic Scattering of ^{6}He+p at 82.3 MeV/nucleon**
FAISAL Jamil-Qureshi, LOU Jian-Ling, YE Yan-Lin, CAO Zhong-Xin, JIANG Dong-Xing, ZHENG Tao, HUA Hui, LI Zhi-Huan, LI Xiang-Qing, GE Yu-Cheng, PANG Dan-Yang, LI Qi-Te, XIAO Jun, LV Lin-Hui, QIAO Rui, YOU Hai-Bo, CHEN Rui-Jiu, LU Fei, Sakurai H, Otsu H, Nishimura M, Sakaguchi S, Baba H, Togano Y, Yoneda K, LI Chen, WANG Shuo, WANG He, LI Kuo-Ang, Nakamura T, Nakayama Y, Kondo Y, Deguchi S, Satou Y, Tshoo K H

ATOMIC AND MOLECULAR PHYSICS

093301 **Dynamics of H_2 in Intense Femtosecond Laser Field**
ZHU Jing-Yi, LIU Ben-Kang, WANG Yan-Qiu, HE Hai-Xiang, WANG Li

093401 **Rovibrational Formation of Ultracold NaH Molecules Induced by an Ultrashort Laser Pulse**
SU Qian-Zhen, YU Jie, NIU Ying-Yu, CONG Shu-Lin

093601 **Photoabsorption Spectra of $(SiO_2)_n$ ($n \leq 5$) Clusters on the Basis of Time-Dependent Density Functional Theory**
LIU Dan-Dan, ZHANG Hong

FUNDAMENTAL AREAS OF PHENOMENOLOGY(INCLUDING APPLICATIONS)

094101 **Influence of Filling Medium of Holes on the Negative-Index Response of Sandwiched Metamaterials**
WANG Xu-Dong, YE Yong-Hong, MA Ji, JIANG Mei-Ping

094102 **Detection of Perfect Cloak in Time Domain**
SU Yu-Huan, SHI Jin-Wei, LIU Da-He, YANG Guo-Jian

094201 **The Axial Spatial Evolution of Optical Field near the Talbot Plane of a Grating**
LU Yun-Qing, LI Pei-Li, ZHENG Jia-Jin

094202 **Effect of Zeroth-Order beam on Azobenzene Polymer Surface Relief Gratings Fabricated by Phase-Mask Method**
WU Wen-Xuan, LUO Yan-Hua, CHENG Xu-Sheng, TIAN Xiu-Jie, QIU Wei-Wei, REN Xi-Feng, ZHU Bing, ZHANG Qi-Jin

094203 **Range-Gated Laser Stroboscopic Imaging for Night Remote Surveillance**
WANG Xin-Wei, ZHOU Yan, FAN Song-Tao, HE Jun, LIU Yu-Liang

094204 **A Two-Stage S-Band Erbium-Doped Fiber Amplifier Based on W-type Erbium-Doped Fiber**
DING Lei, JIA Yuan-Yuan, XING Jun-Bo, ZHANG Zhen, SUN Jian-Jun, LU Ke-Cheng

094205 **Enhanced Surface-Plasmon-Polariton Interference for Nanolithography by a Micro-Cylinder-Lens Array**
LIANG Hui-Min, WANG Jing-Quan, FAN Feng, QIN Ai-Li, ZHANG Chun-Yuan, CHENG Hui

094206 **An Experiment for Generating the 14-Tone Stable Carriers Using Recirculating Frequency Shifter**
TIAN Feng, ZHANG Xiao-Guang, LI Jian-Ping, XI Li-Xia

094207 **Wafer-Level Testable High-Speed Silicon Microring Modulator Integrated with Grating Couplers**
XIAO Xi, ZHU Yu, XU Hai-Hua, ZHOU Liang, HU Ying-Tao, LI Zhi-Yong, LI Yun-Tao, YU Yu-De, YU Jin-Zhong

094208 **High-Frequency Einstein–Podolsky–Rosen Entanglement via Atomic Memory Effects in Four-Wave Mixing**
ZHANG Xue-Hua, HU Xiang-Ming, KONG Ling-Feng, ZHANG Xiu

094209 **An Optical Labeling Scheme with Novel DPSK/PPM Orthogonal Modulation**
ZHOU Rui, XIN Xiang-Jun, WANG Yong-Jun, ZHANG Zi-Xing, YU Chong-Xiu

094301 **Imaging for Borehole Wall by a Cylindrical Linear Phased Array**
ZHANG Bi-Xing, SHI Fang-Fang, WU Xian-Mei, GONG Jun-Jie, ZHANG Cheng-Guang

094302 **Pharmacokinetic Monitoring of Indocyanine Green for Tumor Detection Using Photoacoustic Imaging**
YANG Si-Hua, YIN Guang-Zhi, XING Da

094303 **Effect of Tissue Inhomogeneity on Nonlinear Propagation of Focused Ultrasound**
LIU Zhen-Bo, FAN Ting-Bo, GUO Xia-Sheng, ZHANG Dong

094304 **A Spectral Coupled-Mode Formulation for Sound Propagation around Axisymmetric Seamounts**
LUO Wen-Yu, SCHMIDT Henrik

094701 **Simulation of Non-Newtonian Blood Flow by Lattice Boltzman Method**
JI Yu-Pin, KANG Xiu-Ying, LIU Da-He

PHYSICS OF GASES, PLASMAS, AND ELECTRIC DISCHARGES

095201 **Effects of Perpendicular Thermal Velocities on the Transverse Instability in Electron Phase Space Holes**
WU Ming-Yu, WU Hong, LU Quan-Ming, XUE Bing-Sen

095202 **K-Shell Spectra from CH-Tamped Aluminum Layers Irradiated with Intense Femtosecond Laser Pulses**
XIONG Gang, ZHAO Yang, SHANG Wan-Li, HU Zhi-Min, ZHU Tuo, WEI Min-Xi, YANG Guo-Hong, ZHANG Ji-Yan, YANG Jia-Min

CONDENSED MATTER: STRUCTURE, MECHANICAL AND THERMAL PROPERTIES

096101 **Effect of Zn Interstitials on Enhancing Ultraviolet Emission of ZnO Films Deposited by MOCVD**
ZHONG Ze, SUN Li-Jie, CHEN Xiao-Qing, WU Xiao-Peng, FU Zhu-Xi

096102 **Condensation Behavior of Ag Aggregates on Liquid Surfaces**
ZHANG Xiao-Fei, ZHANG Chu-Hang, LV Neng, XIE Jian-Ping, YE Gao-Xiang

096103 **Small-Angle X-Ray Scattering Study on Nanostructures of Polyimide Films**
LIU Xiao-Xu, YIN Jing-Hua, SUN Dao-Bin, BU Wen-Bin, CHENG Wei-Dong, WU Zhong-Hua

096201 **Structural, Electronic and Elastic Properties of Cubic Perovskites $SrSnO_3$ and $SrZrO_3$ under Hydrostatic Pressure Effect**
SHI Li-Wei, DUAN Yi-Feng, YANG Xian-Qing, QIN Li-Xia

096202 **Preparation of Thermo-Stable Bulk Metallic Glass of $Nd_{60}Cu_{20}Ni_{10}Al_{10}$ by Rapid Compression**
YUAN Chao-Sheng, LIU Xiu-Ru, SHEN Ru, SUN Zhen-Ya, CHEN Bo, LV Shi-Jie, HE Zhu, HU Yun, HONG Shi-Ming

096203 **Collective Modes and Elastic Constants of Liquid $Al_{83}Cu_{17}$ Binary Alloy**
B. Y. Thakore, S. G. Khambholja, P. H. Suthar, N. K. Bhatt, A. R. Jani

096401 **A Three-Component Model Suitable for Natural and Ventilated Cavitation**
JI Bin, LUO Xian-Wu, ZHANG Yao, RAN Hong-Juan, XU Hong-Yuan, WU Yu-Lin

096402 **First-Principles Study of the γ Angle Deformation Path in the Wurtzite-to-Rocksalt Phase Transition in Aluminum Nitride**
CAI Ying-Xiang, XU Rui

096801 **AFM and XPS Study of Glass Surface Coated with Titania Nanofilms by Sol-Gel Method**
JI Guo-Jun, SHI Zhi-Ming

CONDENSED MATTER: ELECTRONIC STRUCTURE, ELECTRICAL, MAGNETIC, AND OPTICAL PROPERTIES

097101 **Tuning Bandgap of Si-C Heterofullerene-Based Aanotubes by H Adsorption**
LI Ji-Ling, YANG Guo-Wei, ZHAO Ming-Wen, LIU Xiang-Dong, XIA Yue-Yuan

097102 **A Density Functional Study of Atomic Carbon Adsorption on δ-Pu(111) Surface**
WEI Hong-Yuan, XIONG Xiao-Ling, SONG Hong-Tao, LUO Shun-Zhong

097401 **Generation and Quantum Interference of Entangled Electron-Hole Pairs in a Hanbury Brown and Twiss Interferometer**
ZHANG Qing-Yun, WANG Bai-Geng, SHEN Rui, XING Ding-Yu

097501 **Soft Magnetic Thin Films FeCoHfO for High-Frequency Noise Suppression Applications**
LU Guang-Duo, ZHANG Huai-Wu, TANG Xiao-Li

097502 **Fabrication, Structural and Magnetic Properties for Aligned MnBi**
LIU Yong-Sheng, ZHANG Jin-Cang, REN Zhong-Ming, GU Min-An, YANG Jing-Jing, CAO Shi-Xun, YANG Zheng-Long

097503 **Magnetization Switching in a Small Disk with Shape Anisotropy**
LÜ Dong-Li, XU Chen

097504 **Modulation of Insulator-Metal Transition Temperature by Visible Light in $La_{7/8}Sr_{1/8}MnO_3$ Thin Film**
HU Ling, SUN Yu-Ping, WANG Bo, LUO Xuan, SHENG Zhi-Gao, ZHU Xue-Bin, SONG Wen-Hai, YANG Zhao-Rong, DAI Jian-Ming

097505 **Structural and Magnetic Properties of $Nd(Fe,Mo)_{12}N_x$ Compounds Produced by Strip-Casting Method**
LIU Shun-Quan, HAN Jing-Zhi, WANG Chang-Sheng, YANG Jin-Bo, DU Hong-Lin, YANG Ying-Chang

097701 **Controllable Ultra Low-*k* by Via-Typed Air Gap with the Better Design Margin for Logic Devices below 45 nm Node**
CHOI Youn-Ok, KIM Sang-Yong

097801 **Polymer Light-Emitting Diode Using Conductive Polymer as the Anode Layer**
LIANG Chun-Jun, ZOU Hui, HE Zhi-Qun, ZHANG Chun-Xiu, LI Dan, WANG Yong-Sheng

CROSS-DISCIPLINARY PHYSICS AND RELATED AREAS OF SCIENCE AND TECHNOLOGY

098101 **Light-Induced Agglomeration and Diffusion of Different Particles with Optical Tweezers**
LI Xue-Cong, SUN Xiu-Dong, LIU Hong-Peng, ZHANG Jian-Long

098102 **Preparation and Characteristics of Nanoscale Diamond-Like Carbon Films for Resistive Memory Applications**
FU Di, XIE Dan, ZHANG Chen-Hui, ZHANG Di, NIU Jie-Bin, QIAN He, LIU Li-Tian

098501 **Spin Injection from Ferromagnetic Metal Directly into Non-Magnetic Semiconductor under Different Injection Currents**
DENG Ning, TANG Jian-Shi, ZHANG Lei, ZHANG Shu-Chao, CHEN Pei-Yi

098502 **Wetting Layer Effect on Optical Gain of Strained CdTe/ZnTe Pyramidal Quantum Dots**
Seoung-Hwan Park, Woo-Pyo Hong

098701 **Synergistic Effect of Auto-Activation and Small RNA Regulation on Gene Expression**
XIONG Li-Ping, MA Yu-Qiang, TANG Lei-Han

098901 **Phase Transition of the Pair Contact Process Model in a Fragmented Network**
HUA Da-Yin, WANG Lie-Yan

GEOPHYSICS, ASTRONOMY, AND ASTROPHYSICS

099701 **The Surface Gravitational Redshift of a Proto Neutron Star**
ZHAO Xian-Feng